

$B \rightarrow K\tau^+\tau^-$ decay in the general two Higgs doublet model

E. O. Iltan *

Physics Department, Middle East Technical University
Ankara, Turkey

Abstract

We study the branching ratio, CP -violating asymmetry, forward-backward asymmetry and the CP -violating asymmetry in the forward-backward asymmetry for the exclusive decay $B \rightarrow K\tau^+\tau^-$ in the two Higgs doublet model with tree level flavor changing neutral currents (model III). We analyse the dependencies of these quantities on the neutral Higgs boson contributions and the CP parameter $\sin\theta$ in the model III. We observe that to determine the neutral Higgs boson effects, the measurements of the forward-backward asymmetry and the CP -violating asymmetry in the forward-backward asymmetry for the decay $B \rightarrow K\tau^+\tau^-$ are promising.

arXiv:hep-ph/0102061v2 31 May 2002

*E-mail address: eiltan@heraklit.physics.metu.edu.tr

1 Introduction

Rare B meson decays, induced by flavor changing neutral current (FCNC) $b \rightarrow s$ transition are the most promising research areas to test the Standard model (SM). Since these decays are induced at loop level in the SM, a comprehensive information can be obtained for the more precise determination of the fundamental parameters, such as Cabbibo-Kobayashi-Maskawa (CKM) matrix elements, leptonic decay constants, etc. Further, they shed light on the physics beyond the SM, such as two Higgs Doublet model (2HDM), Minimal Supersymmetric extension of the SM (MSSM) [1], etc.

Among the rare B-decays, the ones which the SM predicts large branching ratio (Br) become attractive since they are measurable in the near future, in the existing and forthcoming B-factories. The $B \rightarrow Kl^+l^-$, ($l = e, \mu, \tau$) decay, induced by $b \rightarrow sl^+l^-$ transition at the quark level, is one of the candidate. In the literature, there are various experimental studies on this decay [2]-[5]. The 90% C.L. upper limits of $Br(B \rightarrow Kl^+l^-)$ ($l = e, \mu$) have been obtained at the order of the magnitude as 10^{-6} , close the SM predictions.

In [6] -[20], this transition has been investigated extensively in the SM, 2HDM . In these studies, the neutral Higgs boson (NHB) exchange diagrams are not taken into account since the lepton-lepton-Higgs vertices are proportional to the mass of the lepton underconsideration. However, for $l = \tau$ case, the mass m_τ can not be neglected since it is comparable with the b -quark mass and NHB exchange diagrams give considerable contributions to the physical quantities of such channels. In [21], $B \rightarrow K\tau^+\tau^-$ process is studied in the model II 2HDM and the NHB effects are taken into account. It is shown that the Br ratio of the process is enhanced for large $\tan\beta$ values and the NHB contributions become considerable. Recently, this decay has been analysed and the forward backward asymmetry has been studied in the constrained minimal supersymmetric SM [22].

The forward-backward asymmetry A_{FB} and the CP -violating asymmetry A_{CP} are the physical quantities which provide information on the short distance contributions. A_{FB} does not exist in the SM and also in the 2HDM without NHB effects. However, with the addition of these effects, A_{FB} is created and in the model II 2HDM, its numerical value increases with the increasing value of the vertex factor $\tan\beta$ (see [21] for details). The sources of A_{CP} are the complex CKM matrix elements or the Yukawa couplings appear beyond the SM. Since the CP violation in the SM is negligible and no complex coupling exists in the model II (I) version of the 2HDM, one can go further and choose model III version of the 2HDM to get a measurable A_{CP} .

In our work, we study the exclusive $B \rightarrow K\tau^+\tau^-$ decay in the model III. Since the τ lepton mass is comparable with b -quark mass and the new Yukawa coupling $\xi_{N,\tau\tau}^D$, coming from the vertices $\tau\tau h_0$ or $\tau\tau A_0$ can be large, we include the NHB diagrams and test the amount of their contributions. We calculate the Br of the process and observe that it is sensitive to the NHB effects. Second, we get non-zero A_{CP} , at the order of the magnitude 10^{-2} , since the Yukawa couplings in the model III can be taken as complex. A_{FB} appears in the case that the NHB effects are non-zero and, therefore, we study its sensitivity to the Yukawa coupling $\xi_{N,\tau\tau}^D$ and the mass ratio, $\frac{m_{h_0}}{m_{A_0}}$, of the neutral Higgs bosons h_0, A_0 . Finally we calculate the CP -asymmetry in A_{FB} ($A_{CP}(A_{FB})$) and see that it is at the order of the magnitude 10^{-3} . Similar to A_{FB} , $A_{CP}(A_{FB})$ can exist if the NHB effects are non-zero and can be used for testing the contributions beyond the SM.

Note that the theoretical analysis of exclusive decays is more complicated due to the hadronic form factors, which brings an uncertainty in the calculations. The calculation of the physical observables in the hadronic level needs non-perturbative methods to determine the matrix elements of the quark level effective Hamiltonian between the hadronic states. This problem has been studied in the framework of different approaches such as relativistic quark model by the light-front formalism [12], chiral theory [23], three point QCD sum rules method [24], effective heavy quark theory [25] and light cone QCD sum rules [26].

The paper is organized as follows: In Section 2, we calculate the Br, A_{CP}, A_{FB} and $A_{CP}(A_{FB})$ of the exclusive $B \rightarrow K\tau^+\tau^-$ decay. Section 3 is devoted to the analysis of the dependencies of the physical quantities given above on the Yukawa coupling $\bar{\xi}_{N,\tau\tau}^D$, the ratio $\frac{m_{h_0}}{m_{A_0}}$ and the CP parameter $\sin\theta$. In appendix, we give a summary for the model III and the calculation of the matrix element for the inclusive $b \rightarrow sl^+l^-$ decay in this model. Furthermore, we give the explicit forms of the form factors and the parametrizations used in the text.

2 The exclusive $B \rightarrow Kl^+l^-$ decay

The exclusive $B \rightarrow Kl^+l^-$ decay is induced by the inclusive $b \rightarrow sl^+l^-$ process which has been studied in the literature extensively. Recently the $b \rightarrow sl^+l^-$ decay has been handled with the addition the NHB effects in the framework of the general two Higgs doublet model [27]. In the appendix we give a summary of the model underconsideration and present the effective Hamiltonian which is used for the hadronic matrix elements.

The calculation of the physical quantities like Br, A_{FB}, A_{CP} , etc., need the matrix elements

$\langle K | \bar{s} \gamma_\mu (1 + \gamma_5) b | B \rangle$, $\langle K | \bar{s} (1 + \gamma_5) b | B \rangle$ and $\langle K | \bar{s} i \sigma_{\mu\nu} q^\nu (1 + \gamma_5) b | B \rangle$ and they read as [21]

$$\begin{aligned}
\langle K | \bar{s} \gamma_\mu (1 - \gamma_5) b | B \rangle &= (p_B + p_K)_\mu f^+(q^2) + q_\mu f^-(q^2) , \\
\langle K | \bar{s} i \sigma_{\mu\nu} q^\nu (1 + \gamma_5) b | B \rangle &= ((p_B + p_K)_\mu q^2 - q_\mu (m_B^2 - m_K^2)) \frac{f_T(q^2)}{m_B + m_K} , \\
\langle K | \bar{s} (1 + \gamma_5) b | B \rangle &= \frac{1}{m_b} ((m_B^2 - m_K^2) f^+(q^2) + q^2 f^-(q^2)) .
\end{aligned} \tag{1}$$

Here p_B and p_K are four momentum vectors of B and K mesons, $q = p_B - p_K$ is the momentum transfer. Using these form factors, the matrix element of the $B \rightarrow Kl^+l^-$ decay can be written as:

$$\mathcal{M} = -\frac{G\alpha_{em}}{2\sqrt{2}\pi} V_{tb} V_{ts}^* \left\{ [Ap_{K\mu} + Bq_\mu] \bar{\ell} \gamma^\mu \ell + [Cp_{K\mu} + Dq_\mu] \bar{\ell} \gamma^\mu \gamma_5 \ell + F_1 \bar{\ell} \ell + F_2 \bar{\ell} \gamma_5 \ell \right\} \tag{2}$$

where the functions A , B , C , D , F_1 and F_2 are given in Appendix B. Using eq.(2) and making the summation over final lepton polarizations, the double differential decay rate is calculated as:

$$\begin{aligned}
\frac{d\Gamma}{dsdz} &= \frac{G^2 \alpha_{em}^2 |V_{tb} V_{ts}^*|^2 m_B}{2^{12} \pi^5} \left\{ v \sqrt{\lambda} \left(\frac{\lambda}{2} m_B^4 |A|^2 + \frac{1}{2} |C|^2 m_B^2 (\lambda m_B^2 + 16 m_l^2 r) + 2 |F_2|^2 m_B^2 s \right. \right. \\
&+ 8 \text{Re}(D^* F_2) m_B^2 m_l s + 8 |D|^2 m_B^2 m_l^2 s + 4 \text{Re}(C^* F_2) m_B^2 m_l (1 - r - s) \\
&+ 8 \text{Re}(C^* D) m_B^2 m_l^2 (1 - r - s) + 2 |F_1|^2 m_B^2 s v^2 + z (4 \text{Re}(A^* F_1) \sqrt{\lambda} m_B^2 m_l v) \\
&\left. \left. - \frac{z^2}{2} \lambda m_B^4 v^2 (|A|^2 + |C|^2) \right) \right\} \tag{3}
\end{aligned}$$

where $z = \cos\theta$, θ is the angle between the momentum of ℓ lepton and that of B meson in the center of mass frame of the lepton pair, $\lambda = 1 + r^2 + s^2 - 2r - 2s - 2rs$, $v = \sqrt{1 - \frac{4m_l^2}{sm_B^2}}$, $r = \frac{m_K^2}{m_B^2}$ and $s = \frac{q^2}{m_B^2}$. In the light lepton case, namely $l = e, \mu$, the NHB effects are negligible and new Wilson coefficients C_{Q_1} and C_{Q_2} , appearing in the form factors F_1 and F_2 , almost vanish (see [27] for details). However, for τ lepton, the NHB effects can give considerable contributions to the physical quantities Br , A_{FB} , A_{CP} , etc. Even if A_{CP} is possible without these effects, they play the main role in the existence of A_{FB} . Further, $A_{CP}(A_{FB})$ exists when NHB effects are non-zero. Therefore, we concentrate on $A_{CP}(A_{FB})$ in addition to the quantities A_{FB} and A_{CP} . Using the definitions

$$A_{FB} = \frac{\int_0^1 dz \frac{d\Gamma}{dz} - \int_{-1}^0 dz \frac{d\Gamma}{dz}}{\int_0^1 dz \frac{d\Gamma}{dz} + \int_{-1}^0 dz \frac{d\Gamma}{dz}} , \tag{4}$$

$$A_{CP} = \frac{\Gamma - \bar{\Gamma}}{\Gamma + \bar{\Gamma}} \tag{5}$$

we get

$$A_{FB} = \frac{\Phi}{\Omega}, \quad (6)$$

and

$$A_{CP} = \frac{\int ds \left\{ 2A_2 A_3 \lambda^{\frac{3}{2}} v m_B^2 \left(1 - \frac{v^2}{3}\right) \text{Im}(\bar{\xi}_{N,bb}^D) \right\}}{\int ds \Delta}, \quad (7)$$

where

$$\begin{aligned} \Phi = & \int ds \left\{ \lambda v^2 m_B^2 m_\tau (A_3 F_1^{(2)} |\bar{\xi}_{N,bb}^D|^2 + A_2 F_1^{(2)} \text{Im}(\bar{\xi}_{N,bb}^D) \right. \\ & \left. + (A_1 F_1^{(2)} + A_3 F_1^{(1)}) \text{Re}(\bar{\xi}_{N,bb}^D) + A_1 F_1^{(1)} \right\}, \quad (8) \end{aligned}$$

and Ω is obtained from eq. (3) by an integration over z and s of the terms in the curly bracket. Δ in eq. (7) reads as

$$\begin{aligned} \Delta = & v\sqrt{\lambda} \left\{ m_B^2 \lambda (A_1^2 + A_2^2 + C^2) \left(1 - \frac{v^2}{3}\right) + 16 m_\tau^2 (CD\sqrt{\lambda} + (C^2 r + D^2 s)) \right. \\ & + 8 m_\tau F_2^{(1)} (\sqrt{\lambda} C + 2 s D) + 4 s (|F_2|^2 + v^2 |F_1|^2) \\ & + |\bar{\xi}_{N,bb}^D|^2 (m_B^2 \lambda A_3^2 \left(1 - \frac{v^2}{3}\right) + 4 (F_1^{(2)})^2 s v^2) + 2 \text{Re}(\bar{\xi}_{N,bb}^D) (\lambda m_B^2 A_1 A_3 \left(1 - \frac{v^2}{3}\right) + 4 F_1^{(1)} F_1^{(2)} s v^2 \\ & \left. + 4 m_\tau \sqrt{\lambda} C F_2^{(2)} + 8 m_\tau s D F_2^{(2)}) \right\} \quad (9) \end{aligned}$$

The explicit forms of the functions A_i , C , D , $F_j^{(k)}$, $i = 1, 2, 3$; $j, k = 1, 2$ appearing in eqs. (8) and (9) are given in Appendix B.

Finally $A_{CP}(A_{FB})$ can be defined as

$$A_{CP}(A_{FB}) = \frac{A_{FB} - \bar{A}_{FB}}{A_{FB} + \bar{A}_{FB}} \quad (10)$$

where A_{FB} is given in eq. (6) and \bar{A}_{FB} can be calculated by making the replacement $\bar{\xi}_{N,bb}^D \rightarrow \bar{\xi}_{N,bb}^{D*}$ in A_{FB} .

Notice that, during the calculations, we take into account only the second resonance for the LD effects coming from the reaction $b \rightarrow s\psi_i \rightarrow s\tau^+\tau^-$, where $i = 1, \dots, 6$ and divide the integration region for s into two parts : $\frac{4m_\tau^2}{m_B^2} \leq s \leq \frac{(m_{\psi_2} - 0.02)^2}{m_B^2}$ and $\frac{(m_{\psi_2} + 0.02)^2}{m_B^2} \leq s \leq (1 - \sqrt{r})^2$, where $m_{\psi_2} = 3.686 \text{ GeV}$ is the mass of the second resonance

3 Discussion

The model III induces many free parameters, such as $\xi_{N,ij}^{U,D}$ where i, j are flavor indices and they should be restricted using the experimental results. Now, we would like to present the restrictions we use for these parameters, in our numerical calculations. Since the neutral Higgs bosons, h_0 and A_0 , can give a large contribution to the coefficient C_7 which is in contradiction with the CLEO data [28],

$$Br(B \rightarrow X_s \gamma) = (3.15 \pm 0.35 \pm 0.32) 10^{-4} , \quad (11)$$

the couplings $\bar{\xi}_{N,is}^D$ ($i = d, s, b$) and $\bar{\xi}_{N,db}^D$ can be assumed as negligible to be able to reach the conditions $\bar{\xi}_{N,bb}^D \bar{\xi}_{N,is}^D \ll 1$ and $\bar{\xi}_{N,db}^D \bar{\xi}_{N,ds}^D \ll 1$. (see the appendix of [29] for details). Using also the constraints coming from $\Delta F = 2$ mixing, the ρ parameter [30] and the CLEO data we have:

$$\begin{aligned} \bar{\xi}_{N,tc} &\ll \bar{\xi}_{N,tt}^U , \\ \bar{\xi}_{N,ib}^D &\sim 0 , \bar{\xi}_{N,ij}^D \sim 0 , \quad i, j = d, s \text{ quarks} . \end{aligned}$$

This assumption permits us to neglect the contributions coming from primed Wilson coefficients which are related with the chirality flipped partners of the operator set (see [27] for details) since the Yukawa vertices are combinations of $\bar{\xi}_{N,sb}^D$ and $\bar{\xi}_{N,ss}^D$. Finally, we only take into account the Yukawa couplings $\bar{\xi}_{N,tt}^U$, $\bar{\xi}_{N,bb}^D$ and $\bar{\xi}_{N,\tau\tau}^D$. Notice that, for the coupling $\bar{\xi}_{N,\tau\tau}^D$, at first, we do not introduce any constraint and we will try to predict an upper limit by using the present experimental measurements. At this stage we introduce a new parameter θ with the expression

$$\bar{\xi}_{N,tt}^U \bar{\xi}_{N,bb}^{*D} = |\bar{\xi}_{N,tt}^U \bar{\xi}_{N,bb}^{*D}| e^{-i\theta} . \quad (12)$$

Here, it is possible to take both $\bar{\xi}_{N,tt}^U$ and $\bar{\xi}_{N,bb}^D$ or any one of them complex. In our work, we choose $\bar{\xi}_{N,tt}^U$ as real and $\bar{\xi}_{N,bb}^D$ as complex, namely $\bar{\xi}_{N,bb}^D = |\bar{\xi}_{N,bb}^D| e^{i\theta}$. The phase angle θ leads to a substantial enhancement in neutron electric dipole moment and the experimental upper limit on neutron electric dipole moment $d_n < 10^{-25}$ e-cm thus places a upper bound on the couplings: $\frac{1}{m_t m_b} \text{Im}(\bar{\xi}_{N,tt}^U \bar{\xi}_{N,bb}^{*D}) < 1.0$ for $m_{H^\pm} \approx 200$ GeV [31].

In this section, we study the dependencies of the Br , CP asymmetry A_{CP} , forward-backward asymmetry A_{FB} and CP asymmetry in forward-backward asymmetry $A_{CP}(A_{FB})$ of the decay $B \rightarrow K \tau^+ \tau^-$ on the selected parameters of the model III ($\bar{\xi}_{N,\tau\tau}^D$, $\frac{m_{h_0}}{m_{A_0}}$ and phase angle θ). In our analysis we restrict $|C_7^{eff}|$ in the region $0.257 \leq |C_7^{eff}| \leq 0.439$, coming from CLEO measurement (see [32] for details). With this restriction, an allowed region for the parameters

$\bar{\xi}_{N,tt}^U$, $\bar{\xi}_{N,bb}^D$ and θ , is found. Throughout the numerical calculations, we respect this restriction, the constraint for the angle θ due to the experimental upper limit of neutron electric dipole moment and take $|r_{tb}| = \left| \frac{\bar{\xi}_{N,tt}^U}{\bar{\xi}_{N,bb}^D} \right| < 1$, the neutral Higgs mass $m_{H_0} = 100 \text{ GeV}$, charged Higgs mass $m_{H^\pm} = 400 \text{ GeV}$, the scale $\mu = m_b$. Here, we also give the input values used in the calculations, in Table (1).

Parameter	Value
m_c	1.40 (GeV)
m_b	4.80 (GeV)
m_τ	1.78 (GeV)
α_{em}^{-1}	129
λ_t	0.04
$\Gamma_{tot}(B_d)$	$3.96 \cdot 10^{-13}$ (GeV)
m_{B_d}	5.28 (GeV)
m_t	175 (GeV)
m_W	80.26 (GeV)
m_Z	91.19 (GeV)
Λ_{QCD}	0.214 (GeV)
$\alpha_s(m_Z)$	0.117
$\sin\theta_W$	0.2325

Table 1: The values of the input parameters used in the numerical calculations.

In figs. 1 (2) we plot the Br of the decay $B \rightarrow K\tau^+\tau^-$ with respect to the Yukawa coupling $\bar{\xi}_{N,\tau\tau}^D$ (the ratio $\frac{m_{h_0}}{m_{A_0}}$) for $\bar{\xi}_{N,bb}^D = 40 m_b$, $m_{h_0} = 70 \text{ GeV}$, $m_{A_0} = 80 \text{ GeV}$ ($\bar{\xi}_{N,\tau\tau}^D = 10 m_\tau$, $m_{A_0} = 80 \text{ GeV}$). The Br is restricted in the region between solid lines (dashed lines) for $C_7^{eff} > 0$ ($C_7^{eff} < 0$). Fig. 1 shows that Br is sensitive to the NHB effects especially for $C_7^{eff} > 0$ case. For increasing values of $\bar{\xi}_{N,\tau\tau}^D$, Br can take even two orders of magnitude larger values compared to the case where no NHB is taken into account. From this figure, it is possible to predict the upper limit of the coupling $\bar{\xi}_{N,\tau\tau}^D$, $\bar{\xi}_{N,\tau\tau}^D < 20 \text{ GeV}$, respecting the experimental upper limit, $Br(B \rightarrow Kl^+l^-) < 0.5 \times 10^{-6}$, ($l = e, \mu$) [5], with the assumption that the $Br(B \rightarrow K\tau^+\tau^-)$ is not so much different than the previous one. For $C_7^{eff} < 0$ the possible numerical values lie near 10^{-7} and the Br is not sensitive to the NHB effects. Note that, the Br in the SM is $1.06 \cdot 10^{-7}$ and in the model III without NHB effects are between upper and lower limits $(1.05 - 1.08) \cdot 10^{-7}$ ($(0.95 - 0.97) \cdot 10^{-7}$) for $C_7^{eff} > 0$ ($C_7^{eff} < 0$). As shown in Fig. 2, the Br is also sensitive to the ratio $\frac{m_{h_0}}{m_{A_0}}$ for $C_7^{eff} > 0$ case and it increases for the larger values of the ratio. Furthermore, the experimental value of the $Br(B \rightarrow Kl^+l^-)$ shows that the mass values of the neutral Higgs bosons h_0 and A_0 are not far.

Fig. 3 is devoted to the $\sin\theta$ dependence of A_{CP} including NHB effects. Here, A_{CP} is restricted in the region between solid lines (dashed lines) for $C_7^{eff} > 0$ ($C_7^{eff} < 0$). It is at the order of the magnitude 10^{-3} and increases with the increasing values of the parameter $\sin\theta$ as it should be. For $C_7^{eff} > 0$, the possible values of A_{CP} have the same sign (here minus), however for $C_7^{eff} < 0$ it can vanish or it can have both signs. We also present the $\sin\theta$ dependence of A_{CP} without NHB effects, in Fig. 4. For this case A_{CP} is greater as a magnitude and the restriction region is larger compared to the previous one, especially for $C_7^{eff} > 0$. As it can be seen from eq. (7), the addition of NHB effects reduces the magnitude of the A_{CP} since NHB contributions enter into expression in the denominator but not in the numerator.

In Figs. 5 (6), we plot the A_{FB} of the decay $B \rightarrow K\tau^+\tau^-$ with respect to the Yukawa coupling $\bar{\xi}_{N,\tau\tau}^D$ (the ratio $\frac{m_{h_0}}{m_{A_0}}$) for $\bar{\xi}_{N,bb}^D = 40 m_b$, $m_{h_0} = 70 GeV$, $m_{A_0} = 80 GeV$ ($\bar{\xi}_{N,\tau\tau}^D = 10 m_\tau$, $m_{A_0} = 80 GeV$). A_{FB} is restricted in the region between solid lines (dashed lines) for $C_7^{eff} > 0$ ($C_7^{eff} < 0$). Since A_{FB} appears only with the NHB effects, it is a good candidate for testing the existence of them. A_{FB} is at the order of the magnitude 10^{-2} and increases with the increasing values of $\bar{\xi}_{N,\tau\tau}^D$ for $C_7^{eff} < 0$ as shown in Fig. 5. The behavior of A_{FB} is different for $C_7^{eff} > 0$ since it slightly decreases when $\bar{\xi}_{N,\tau\tau}^D$ increases. In addition to this, A_{FB} is sensitive the ratio $\frac{m_{h_0}}{m_{A_0}}$ for $C_7^{eff} > 0$ and increases as a magnitude with the decreasing ratio (see Fig. 6). However for $C_7^{eff} < 0$ A_{FB} is not sensitive to the ratio $\frac{m_{h_0}}{m_{A_0}}$. Further, it has negative sign for both $C_7^{eff} > 0$ and $C_7^{eff} < 0$.

Finally, we present the CP violating asymmetry in A_{FB} ($A_{CP}(A_{FB})$) in Figs. 7 and 8 since this parameter exists when NHB effects are non-zero and can play an important role in the determination of those effects. Fig. 7 shows $\bar{\xi}_{N,\tau\tau}^D$ dependence of $A_{CP}(A_{FB})$ for $C_7^{eff} > 0$ (lies between solid lines) and $C_7^{eff} < 0$ (lies between dashed lines). This quantity is not so much sensitive to $\bar{\xi}_{N,\tau\tau}^D$ and can be at the order of the magnitude 10^{-4} for $C_7^{eff} < 0$. It can have both signs or can vanish for this case. For $C_7^{eff} > 0$, the numerical value of $A_{CP}(A_{FB})$ can increase up to 10^{-3} . Here, the SM Higgs H_0 part of the NHB effects causes to have large values for $A_{CP}(A_{FB})$ and the part which contains neutral Higgs bosons beyond enters into expression destructively. Fig. 8 represents $\sin\theta$ dependence of $A_{CP}(A_{FB})$. As shown in this figure, the possible values of $A_{CP}(A_{FB})$ for $C_7^{eff} > 0$ have the same sign and they are non-zero for nonzero $\sin\theta$, however for $C_7^{eff} < 0$ $A_{CP}(A_{FB})$ can vanish or exist with both signs.

Now we would like to present our conclusions.

- The Br of the exclusive process $B \rightarrow K\tau^+\tau^-$ is at the order of the magnitude 10^{-7} for the SM and model III without the NHB effects. However, including the NHB effects and

taking large values of the neutral coupling $\bar{\xi}_{N,\tau\tau}^D$, it is possible to enhance the Br more than one orders of magnitude compared to the one calculated in the SM.

- It would be possible to predict the upper limit of the coupling $\bar{\xi}_{N,\tau\tau}^D, \bar{\xi}_{N,\tau\tau}^D < 20 GeV$, respecting the experimental upper limit, $Br(B \rightarrow Kl^+l^-) < 0.5 \times 10^{-6}$, ($l = e, \mu$) [5].
- Using the complex Yukawa coupling $\bar{\xi}_{N,bb}^D$ it is possible to get a CP violating asymmetry A_{CP} at the order of the magnitude 10^{-3} , which is a measurable quantity. With the addition of NHB effects the magnitude of A_{CP} decreases.
- A_{FB} is another physical quantity which exists when the NHB effects are non-zero. The calculations show that A_{FB} is at the order of the magnitude 10^{-2} and the experimental measurement of this quantity can give strong evidence about the existence of NHB effects and the physics beyond the SM.
- Finally, the CP asymmetry in A_{FB} can appear also with the NHB effects and it is another physical quantity which can be used for testing the existence of the NHB effects. We calculate this quantity at the order of the magnitude 10^{-3} and its experimental measurement can give important clues about physics beyond the SM

Therefore, experimental investigations of these physical quantities ensure a crucial test for the new physics beyond the SM.

4 Acknowledgement

This work was supported by Turkish Academy of Sciences (TUBA/GEBIP).

Appendix

A The model III and the inclusive $b \rightarrow s\tau^+\tau^-$ decay

In the SM and model I and II 2HDM, the flavour changing neutral current at tree level is forbidden. However, such currents are permitted in the general 2HDM, so called model III and it brings new parameters, i.e. Yukawa couplings, into the theory. These couplings are responsible for the interaction of quarks and leptons with gauge bosons, namely, the Yukawa interaction and in this general case it reads as

$$\begin{aligned} \mathcal{L}_Y &= \eta_{ij}^U \bar{Q}_{iL} \tilde{\phi}_1 U_{jR} + \eta_{ij}^D \bar{Q}_{iL} \phi_1 D_{jR} + \xi_{ij}^U \bar{Q}_{iL} \tilde{\phi}_2 U_{jR} + \xi_{ij}^D \bar{Q}_{iL} \phi_2 D_{jR} \\ &+ \eta_{ij}^D \bar{l}_{iL} \phi_1 E_{jR} + \xi_{ij}^D \bar{l}_{iL} \phi_2 E_{jR} + h.c. , \end{aligned} \quad (13)$$

where L and R denote chiral projections $L(R) = 1/2(1 \mp \gamma_5)$, ϕ_k , for $k = 1, 2$, are the two scalar doublets, Q_{iL} (l_{iL}) are quark (lepton) doublets, U_{jR} and D_{jR} are quark singlets, E_{jR} are lepton singlets, $\eta_{ij}^{U,D}$, and $\xi_{ij}^{U,D}$ are the matrices of the Yukawa couplings. The Flavor changing (FC) part of the interaction is given by

$$\mathcal{L}_{Y,FC} = \xi_{ij}^U \bar{Q}_{iL} \tilde{\phi}_2 U_{jR} + \xi_{ij}^D \bar{Q}_{iL} \phi_2 D_{jR} + \xi_{ij}^D \bar{l}_{iL} \phi_2 E_{jR} + h.c. . \quad (14)$$

With the choice of ϕ_1 and ϕ_2

$$\phi_1 = \frac{1}{\sqrt{2}} \left[\begin{pmatrix} 0 \\ v + H_0 \end{pmatrix} + \begin{pmatrix} \sqrt{2}\chi^+ \\ i\chi^0 \end{pmatrix} \right] ; \phi_2 = \frac{1}{\sqrt{2}} \begin{pmatrix} \sqrt{2}H^+ \\ H_1 + iH_2 \end{pmatrix} . \quad (15)$$

and the vacuum expectation values,

$$\langle \phi_1 \rangle = \frac{1}{\sqrt{2}} \begin{pmatrix} 0 \\ v \end{pmatrix} ; \langle \phi_2 \rangle = 0 , \quad (16)$$

the SM and beyond can be decoupled. In eq.(14) the couplings $\xi^{U,D}$ for the FC charged interactions are

$$\begin{aligned} \xi_{ch}^U &= \xi_{neutral} V_{CKM} , \\ \xi_{ch}^D &= V_{CKM} \xi_{neutral} , \end{aligned} \quad (17)$$

where $\xi_{neutral}^{U,D}$ ¹ is defined by the expression

$$\xi_N^{U,D} = (V_L^{U,D})^{-1} \xi^{U,D} V_R^{U,D} . \quad (18)$$

¹In all next discussion we denote $\xi_{neutral}^{U,D}$ as $\xi_N^{U,D}$.

Here the charged couplings appear as linear combinations of neutral couplings multiplied by V_{CKM} matrix elements (see [30] for details).

Now, we would like to present the procedure to calculate the matrix element for the inclusive $b \rightarrow s\tau^+\tau^-$ decay briefly:

- Integrating out the heavy degrees of freedom, namely t quark, W^\pm , charged Higgs boson H^\pm , and neutral Higgs bosons H_0, H_1, H_2 bosons in the present case and obtaining the effective theory. Note that H_1 and H_2 are the same as the mass eigenstates h_0 and A_0 in the model III respectively, due to the choice given by eq. (15).
- Taking into account the QCD corrections through matching the full theory with the effective low energy one at the high scale $\mu = m_W$ and evaluating the Wilson coefficients from m_W down to the lower scale $\mu \sim O(m_b)$.

In the 2HDM, neutral Higgs particles bring new contributions to the matrix element of the process $b \rightarrow s\tau^+\tau^-$ (see [27]) since they enter in the expressions with the mass of τ lepton or related Yukawa coupling $\bar{\xi}_{N,\tau\tau}^D$. Besides, there exist additional operators which are the flipped chirality partners of the former ones in the model III. However, the effects of the latter are negligible since the corresponding Wilson coefficients are small (see Discussion part). Therefore, the effective Hamiltonian relevant for the process $b \rightarrow s\tau^+\tau^-$ is

$$\mathcal{H}_{eff} = -4\frac{G_F}{\sqrt{2}}V_{tb}V_{ts}^* \left\{ \sum_i C_i(\mu)O_i(\mu) + \sum_i C_{Q_i}(\mu)Q_i(\mu) \right\}, \quad (19)$$

where O_i are current-current ($i = 1, 2$), penguin ($i = 3, \dots, 6$), magnetic penguin ($i = 7, 8$) and semileptonic ($i = 9, 10$) operators. Here, $C_i(\mu)$ are Wilson coefficients normalized at the scale μ . The additional operators $Q_i(i = 1, \dots, 10)$ are due to the NHB exchange diagrams and $C_{Q_i}(\mu)$ are their Wilson coefficients (see [27] for the existing operators and the corresponding Wilson coefficients).

B The form factors and the functions appearing in the expressions

We parametrize the functions A, F_1 and F_2 as

$$\begin{aligned} A &= A_1 + i A_2 + \bar{\xi}_{N,bb}^D A_3 \\ F_1 &= F_1^{(1)} + \bar{\xi}_{N,bb}^D F_1^{(2)} \\ F_2 &= F_2^{(1)} + \bar{\xi}_{N,bb}^D F_2^{(2)} \end{aligned} \quad (20)$$

with

$$\begin{aligned}
A_1 &= 2 \operatorname{Re}(C_9^{eff}) f^+ - \frac{4m_b f_T}{m_B + m_K} C_7^{eff} \Big|_{\bar{\xi}_{N,bb}^D \rightarrow 0} , \\
A_2 &= 2 \operatorname{Im}(C_9^{eff}) f^+ , \\
A_3 &= -\frac{4m_b f_T}{m_B + m_K} \frac{1}{m_b m_t} \bar{\xi}_{N,tt}^U (\eta^{\frac{16}{23}} K_2(y_t) + \frac{8}{3} (\eta^{\frac{14}{23}} - \eta^{\frac{16}{23}}) G_2(y_t)) , \\
F_1^{(1)} &= \eta^{-12/23} \frac{(m_B^2 - m_K^2) f^+ + m_B^2 s f^-}{m_b} \int_0^1 dx \int_0^{1-x} dy (C_{Q_1}^{H_0} ((\bar{\xi}_{N,tt}^U)^2) + C_{Q_1}^{H_0} (\bar{\xi}_{N,tt}^U)) \\
&\quad + C_{Q_1}^{H_0} (g^4) + C_{Q_1}^{h_0} ((\bar{\xi}_{N,tt}^U)^3) + C_{Q_1}^{h_0} ((\bar{\xi}_{N,tt}^U)^2) + C_{Q_1}^{h_0} (\bar{\xi}_{N,tt}^U) , \\
F_1^{(2)} &= \eta^{-12/23} \frac{(m_B^2 - m_K^2) f^+ + m_B^2 s f^-}{m_b \bar{\xi}_{N,bb}^D} \int_0^1 dx \int_0^{1-x} dy C_{Q_1}^{h_0} (\bar{\xi}_{N,bb}^D) , \\
F_2^{(1)} &= \eta^{-12/23} \frac{(m_B^2 - m_K^2) f^+ + m_B^2 s f^-}{m_b} \int_0^1 dx \int_0^{1-x} dy (C_{Q_2}^{A_0} ((\bar{\xi}_{N,tt}^U)^3) + C_{Q_2}^{A_0} ((\bar{\xi}_{N,tt}^U)^2) \\
&\quad + C_{Q_2}^{A_0} (\bar{\xi}_{N,tt}^U)) , \\
F_2^{(2)} &= \eta^{-12/23} \frac{(m_B^2 - m_K^2) f^+ + m_B^2 s f^-}{m_b \bar{\xi}_{N,bb}^D} \int_0^1 dx \int_0^{1-x} dy C_{Q_2}^{A_0} (\bar{\xi}_{N,bb}^D) , \tag{21}
\end{aligned}$$

where the formfactors f^+ , f^- and f_T are calculated in the framework of the light cone QCD sum rules and represented in the pole forms as [26]

$$\begin{aligned}
f^+ &= \frac{0.29}{1 - \frac{m_B^2 s}{23.7}} , \\
f^- &= -\frac{0.21}{1 - \frac{m_B^2 s}{24.3}} , \\
f^T &= -\frac{0.31}{1 - \frac{m_B^2 s}{23}} .k \tag{22}
\end{aligned}$$

The other functions B , C and D appearing in eq. (2) are

$$\begin{aligned}
B &= C_9^{eff} (f^- + f^+) + C_7^{eff} \frac{2m_b f_T}{s} \frac{(1 - r - s)}{m_B + m_K} , \\
C &= 2C_{10} f^+ , \\
D &= C_{10} (f^- + f^+) . \tag{23}
\end{aligned}$$

References

- [1] J. L. Hewett, in Proc. of the 21st Annual SLAC Summer Institute, ed. L. De Porcel and C. Dunwoode, SLAC-PUB-6521 (1994)

- [2] The Babar Collaboration, *hep-ex/0107026*.
- [3] CLEO Collaboration, *Phys. Rev. Lett.* **87** (2001) 181803.
- [4] The Belle Collaboration, *Phys. Rev. Lett.* **88** (2002) 029801.
- [5] The Babar Collaboration, *hep-ex/0201008*.
- [6] W. -S. Hou, R. S. Willey and A. Soni, *Phys. Rev. Lett.* **58** (1987) 1608.
- [7] N. G. Deshpande and J. Trampetic, *Phys. Rev. Lett.* **60** (1988) 2583.
- [8] C. S. Lim, T. Morozumi and A. I. Sanda, *Phys. Lett.* **B218** (1989) 343.
- [9] B. Grinstein, M. J. Savage and M. B. Wise, *Nucl. Phys.* **B319** (1989) 271.
- [10] C. Dominguez, N. Paver and Riazuddin, *Phys. Lett.* **B214** (1988) 459.
- [11] N. G. Deshpande, J. Trampetic and K. Ponose, *Phys. Rev.* **D39** (1989) 1461.
- [12] W. Jaus and D. Wyler, *Phys. Rev.* **D41** (1990) 3405.
- [13] P. J. O'Donnell and H. K. Tung, *Phys. Rev.* **D43** (1991) 2067.
- [14] N. Paver and Riazuddin, *Phys. Rev.* **D45** (1992) 978.
- [15] A. Ali, T. Mannel and T. Morozumi, *Phys. Lett.* **B273** (1991) 505.
- [16] A. Ali, G. F. Giudice and T. Mannel, *Z. Phys.* **C67** (1995) 417.
- [17] C. Greub, A. Ioanmissian and D. Wyler, *Phys. Lett.* **B346** (1995) 145;
D. Liu *Phys. Lett.* **B346** (1995) 355;
G. Burdman, *Phys. Rev.* **D52** (1995) 6400;
Y. Okada, Y. Shimizu and M. Tanaka *Phys. Lett.* **B405** (1997) 297.
- [18] A. J. Buras and M. Münz, *Phys. Rev.* **D52** (1995) 186.
- [19] N. G. Deshpande, X. -G. He and J. Trampetic, *Phys. Lett.* **B367** (1996) 362.
- [20] C. Q. Geng, C. P Kao, *Phys. Rev.* **D54** (1996) 5636.
- [21] T. M. Aliev, A. Özpineci, M.Savcı, and H. Koru *J. Phys.* **G24** (1998) 49 . [A
- [22] D. A. Demir, K. A. Olive and M. B. Voloshin, *hep-ph/0204119*

- [23] R. Casalbuoni, A. Deandra, N. Di Bartolemo, R. Gatto and G. Nardulli, *Phys. Lett.* **B312** (1993) 315.
- [24] P. Colangelo, F. De Fazio, P. Santorelli and E. Scrimieri, *Phys. Rev.* **D53** (1996) 3672.
- [25] W. Roberts, *Phys. Rev.* **D54** (1996) 863.
- [26] T. M. Aliev, A. Özpineci and M.Savcı, *Phys. Lett.* **B400** (1997) 194 .
- [27] E. Iltan and G. Turan, *Phys. Rev.* **D63** (2001) 115007.
- [28] M. S. Alam, CLEO Collaboration, to appear in ICHEP98 Conference (1998)
- [29] T. M. Aliev, and E. Iltan, *Phys. Rev.* **D58** (1998) 095014.
- [30] D. Atwood, L. Reina and A. Soni, *Phys. Rev.* **D55** (1997) 3156.
- [31] D. B. Chao, K. Cheung and W. Y. Keung, *Phys. Rev.* **D59** (1999) 115006.
- [32] T. M. Aliev, E. Iltan *J. Phys.* **G25** (1999) 989.

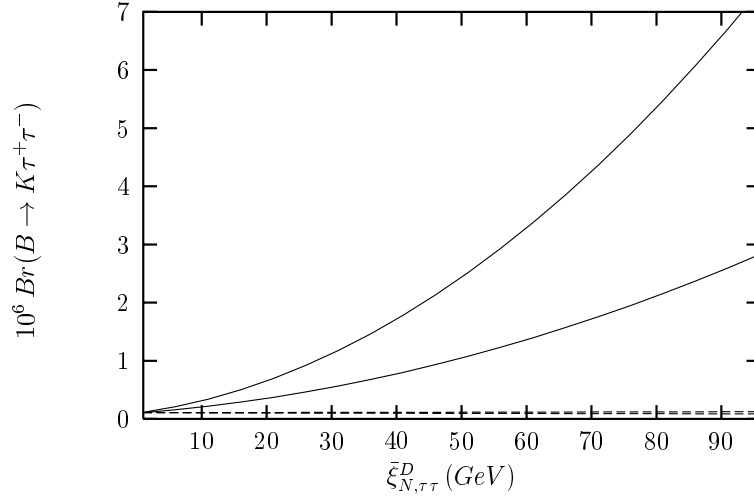


Figure 1: Br as a function of $\bar{\xi}_{N,\tau\tau}^D$, for fixed $\bar{\xi}_{N,bb}^D = 40 m_b$, $m_{h_0} = 70 \text{ GeV}$, $m_{A_0} = 80 \text{ GeV}$ and $\sin\theta = 0$. Here Br lies in the region bounded by solid (dashed) lines for $C_7^{eff} > 0$ ($C_7^{eff} < 0$).

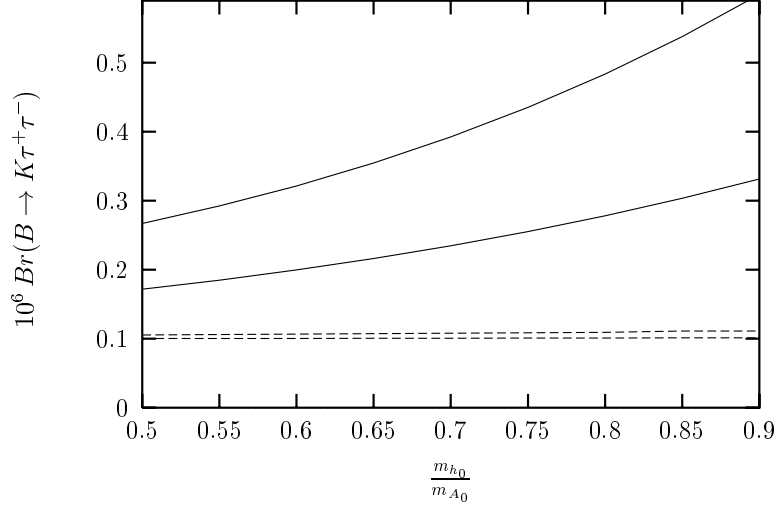


Figure 2: Br as a function of $\frac{m_{h_0}}{m_{A_0}}$, for fixed $m_{A_0} = 80 \text{ GeV}$, $\bar{\xi}_{N,bb}^D = 40 m_b$, $\bar{\xi}_{N,\tau\tau}^D = 10 m_\tau$ and $\sin\theta = 0$. Here Br lies in the region bounded by solid (dashed) lines for $C_7^{eff} > 0$ ($C_7^{eff} < 0$).

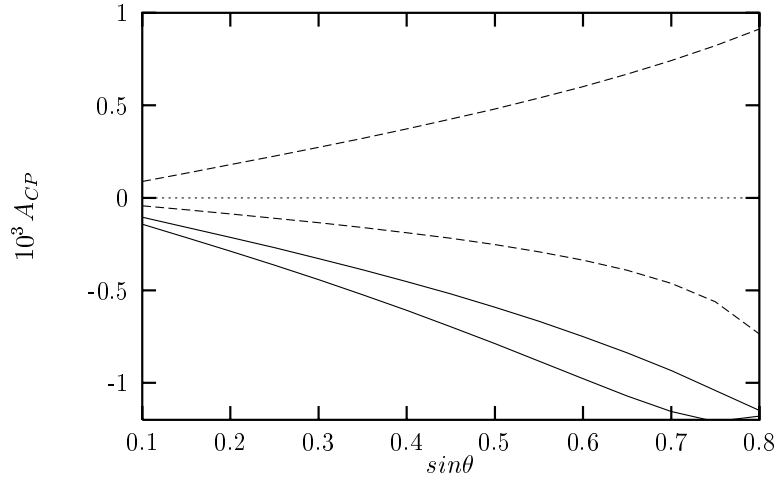


Figure 3: A_{CP} as a function of $\sin\theta$, for fixed $\bar{\xi}_{N,\tau\tau}^D = 10 m_\tau$, $\bar{\xi}_{N,bb}^D = 40 m_b$, $m_{h_0} = 70 \text{ GeV}$, and $m_{A_0} = 80 \text{ GeV}$. Here A_{CP} lies in the region bounded by solid (dashed) lines for $C_7^{eff} > 0$ ($C_7^{eff} < 0$).

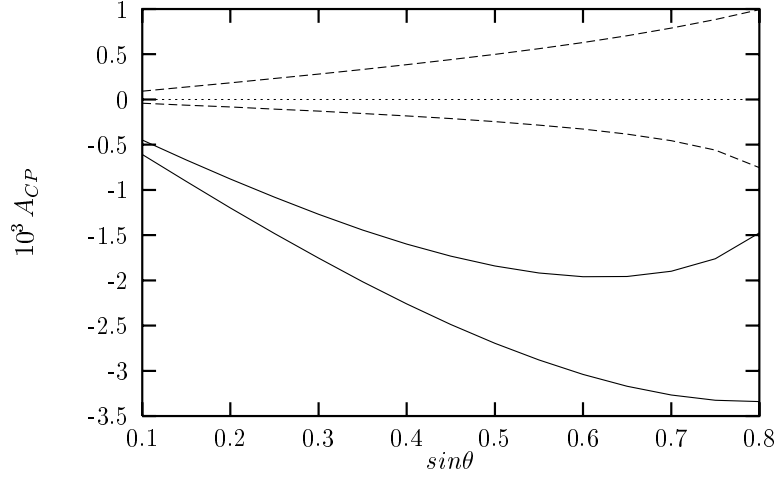


Figure 4: The same as Fig. 3 but without NHB effects.

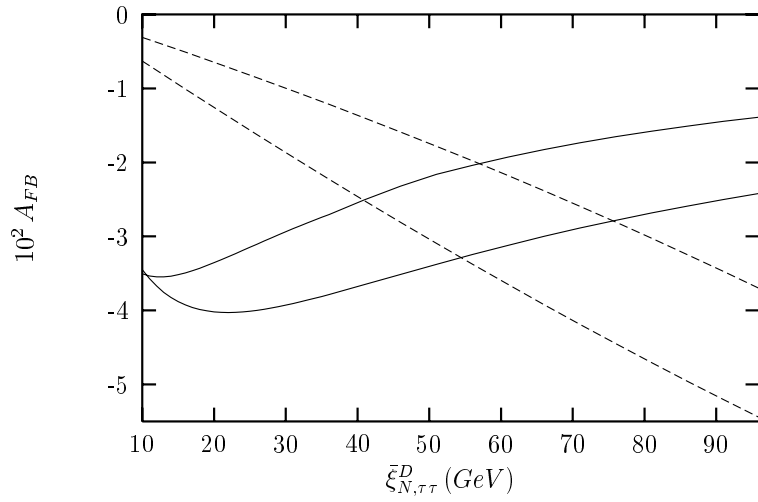


Figure 5: The same as Fig. 1, but for A_{FB} as a function of $\bar{\xi}_{N,\tau\tau}^D$.

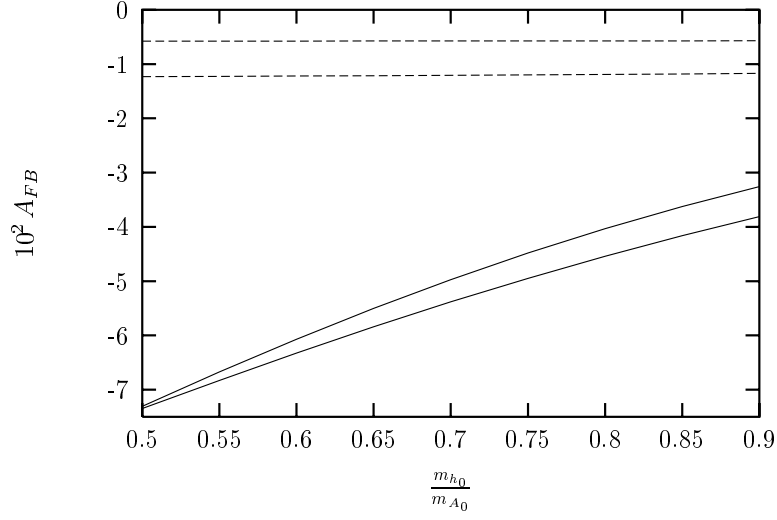


Figure 6: The same as Fig. 2, but for A_{FB} as a function of $\frac{m_{h_0}}{m_{A_0}}$.

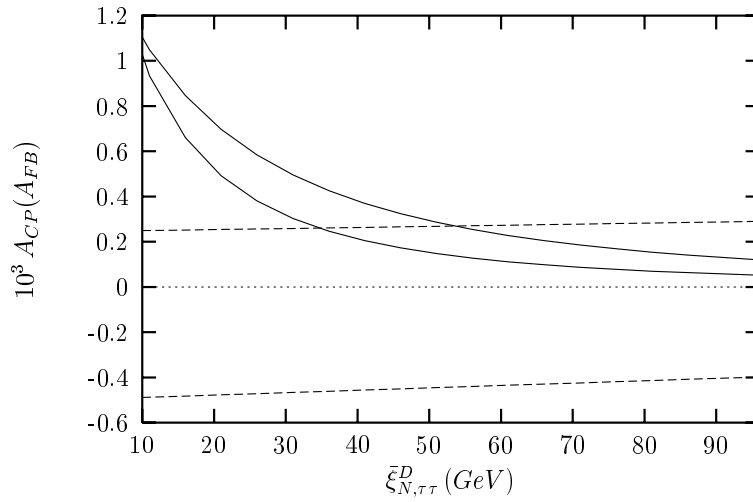


Figure 7: The same as Fig. 1, but for $A_{CP}(A_{FB})$ as a function of $\bar{\xi}_{N,\tau\tau}^D$ and $\sin\theta = 0.5$

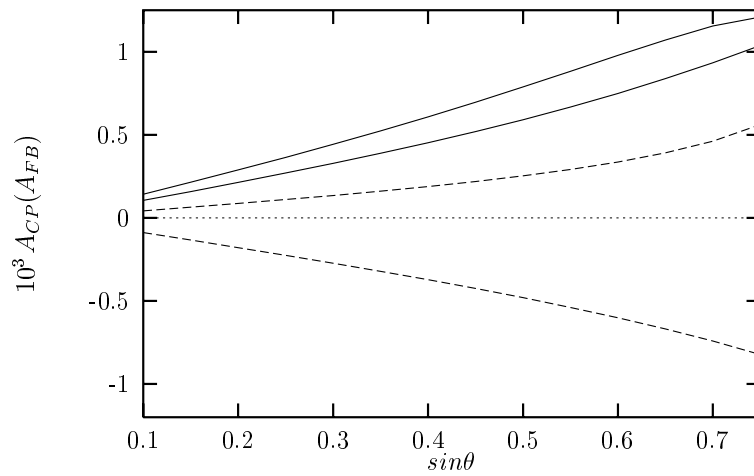


Figure 8: The same as Fig. 3, but for $A_{CP}(A_{FB})$ as a function of $\sin\theta$.